NUMERICAL STUDY ON THE INFLUENCE OF IN-DEPTH RADIATION IN THE PYROLYSIS OF MEDIUM DENSITY FIBREBOARD

Guoxiang Zhao*, Tarek Beji, Davood Zeinali, Bart Merci
Dept. of Flow, Heat and Combustion Mechanics, Ghent University, Ghent, Belgium

ABSTRACT

In order to accurately predict the flame spread along a combustible wall, a better understanding of the burning behaviour of a material exposed to external radiation is required. This work focuses on simulating the pyrolysis behaviour of the Medium Density Fiberboard (MDF) material. The numerical simulation tool used in this study is the Fire Dynamics Simulator (FDS 6.2.0). A one-dimensional heat transfer solver that includes in-depth radiation is employed. The simulation results were compared with the experimental data, including the mass loss rate, and the surface temperature. The base case does not show satisfactory results for the time to reach the first peak and the value of that peak in the mass loss rate curve when compared to experimental data. The influence of the material properties and model parameters on the pyrolysis behaviour of MDF has been investigated in detail through a sensitivity analysis. For the considered range of parameters, the most significant influence on the time to the first peak comes from the emissivity, followed by the thermal conductivity, specific heat, and moisture content. For the peak mass loss rate, the most significant influence comes from the absorption coefficient, followed by the through-thickness density, the moisture content, and the specific heat. Only when proper values of these parameters were employed in the simulation, the onset of the pyrolysis process can be reasonably predicted. Through a simple trial and error procedure, a set of 'optimized' values of parameters including the in-depth absorption coefficient of char was obtained, which results in better agreement with experimental data.

1. INTRODUCTION

In the configuration of flame spread along a vertical combustible wall, thermal radiation of gas-phase combustion products drives the pyrolysis process by heating the unpyrolyzed material surface to pyrolysis temperature. Therefore, a better understanding of the burning behaviour of a material exposed to external radiation is required. A lot of effort has been devoted to study the burning behaviour of both charring and non-charring materials in the literature [1-5]. It has been demonstrated that numerical methods are suitable to predict the mass loss rate and burning rate for non-charring materials. However, the predicted results highly depend on the value of the input parameters, which include the thermal properties of the material and other parameters used in the pyrolysis model (e.g., kinetic parameters).

In-depth absorption of radiation has been reported to have a large influence on the burning behaviour of non-charring materials such as PMMA (Polymethylmethacrylate) [6-7]. However, the influence on the burning behaviour of charring materials (e.g., wood-based products) has not been extensively studied, presumably because opaque conditions are assumed. Nevertheless, in the case of cracks or delamination, in-depth-like radiation absorption may occur.

In this paper we present numerical simulations of MDF pyrolysis using a one-dimensional heat transfer solver that includes in-depth radiation transport. A one-step finite rate reaction is assumed; the virgin material is converted to char and the rest is released as pyrolysate. The values of the kinetic parameters and char yield are estimated from Thermogravimetric Analysis (TGA) test results reported in [3]. The thermal properties of virgin MDF and char are taken from the literature. More details on the pyrolysis model are

provided in the numerical model section.

The goal of this study is to predict the burning behaviour of MDF, with an emphasis on the importance of in-depth radiation. The numerical simulation tool used in this study is the Fire Dynamics Simulator (FDS 6.2.0), which is developed and maintained by the National Institute of Standards and Technology (NIST) [8]. The physical processes occurring in the solid phase are solved as a one-dimensional problem with a one-step pyrolysis model. The input parameters include the material properties, kinetic parameters (e.g., pre-exponential factor and activation energy) properties and boundary conditions. A sensitivity analysis is conducted to study the influence of these input parameters on the burning behaviour of MDF.

2. EXPERIMENTAL CONFIGURATIONS

Small scale tests have been conducted by FM Global in the Fire Propagation Apparatus (FPA) [2]. The MDF sample used in these tests are manufactured by SPANOLUX [9]. Figure 1 shows the schematic of this configuration. The back side of the sample is actually insulated with Cotronics ceramic paper, which has a relatively low thermal conductivity (0.028 W/(m·K)). That is why an adiabatic boundary condition is used in the numerical simulations. The dimensions of the sample are 80 mm× 80 mm × 18.4 mm (height).

The tests have been conducted in nitrogen atmosphere in order to eliminate uncertainties related to gas-phase combustion. During these tests, the mass loss rate, surface and back side temperatures have been measured under three constant external heat fluxes, namely 25, 50, and 100 kW/m^2. More details can be found in reference [2].

Figure 1 Schematic of the MDF sample in FPA test.

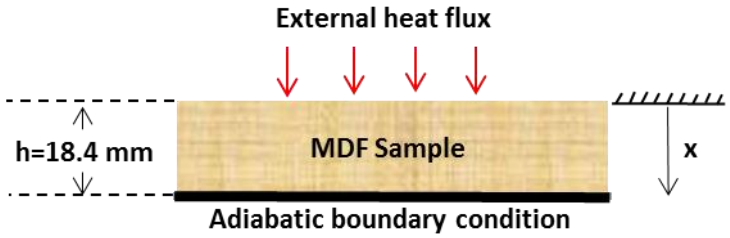

3. NUMERICAL MODEL

As mentioned in the introduction, numerical techniques have been employed in this study. In this section, the numerical model and input parameters will be discussed in detail.

3.1 Pyrolysis model

The pyrolysis process is simplified as a one-step finite rate reaction. Only three species are treaded here, namely the virgin solid, char, and pyrolysate. For the solid reaction, the virgin is converted to char and releases pyrolysate, as shown in the following reaction.

$$\text{Virgin} \rightarrow (1-v_c)\,\text{Pyrolysate} + v_c\,\text{Char} \qquad [1]$$

where v_c is the yield of char. Since neither shrinkage nor swelling is modelled here (i.e., constant volume), the yield of char can be calculated as $v_c = \rho_c / \rho_v$, where ρ_v and ρ_c are the densities of respectively the virgin and the char.

With this one-step pyrolysis model, the pyrolysis rate of the sample is calculated using a temperature-dependent Arrhenius expression. The mass conservation equations for virgin and char are expressed as follows:

$$\frac{dY_v}{dt} = -AY_v \exp(-\frac{E}{RT}) \quad [2]$$

$$\frac{dY_c}{dt} = -v_c \frac{dY_v}{dt} \quad [3]$$

where Y_v and Y_c are the mass fractions of virgin and char respectively. The initial value of the virgin mass fraction $Y_{v,0}$ is equal to 1. T is the temperature (in Kelvin) within the solid. R is the universal gas constant, 8.314J mol^{-1} K^{-1}. A is the Arrhenius pre-exponential factor, with units of s^{-1}. E is the activation energy, with units of kJ/kmol.

It should be noted that the kinetic parameters are not available for most real materials. In practice, the values of A, E and v_c can be obtained from bench-scale measurements like TGA under an inert atmosphere. These measurements consist of heating the sample at a fixed rate, $\dot{T}$, and measuring the residual mass and the reaction rate (in s^{-1} or min^{-1}) as a function of the temperature (see example in Fig. 2).

Figure 2 Typical TGA results for MDF pyrolysis at a heating rate of $\dot{T}$ = 5 K/min [8]. (a) black line represents the normalized residual mass (b) blue line represents the reaction rate

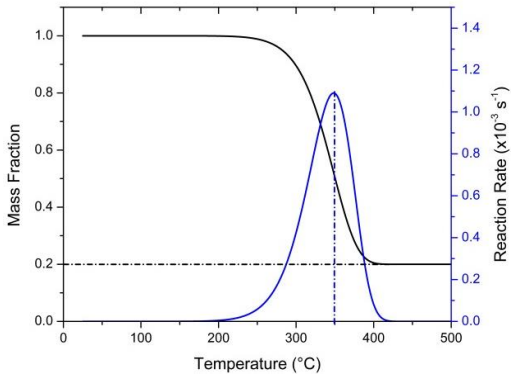

The results in Fig. 2 show a residual mass of 21% at high temperatures. This indicates that we can take $v_c = 0.21$. The peak reaction rate $\gamma_p = 0.0011 \text{s}^{-1}$ occurs at a temperature $T_p = 350$ °C. The blue curve in Fig. 2 can also be characterised by a pyrolysis range (ΔT), which is the approximate width of this curve (in degree Celsius or Kelvin). Assuming a triangular shape for the curve, this width can be estimated as [8]:

$$\Delta T = (1 - v_c) Y_{v,0} \frac{2\dot{T}}{\gamma_p} \quad [4]$$

Based on the obtained value of T_p , ΔT and v_c from TGA tests, the kinetics parameters E and A can be estimated as [8]:

$$E = \frac{2e(1 - v_c) R T_p}{\Delta T} \quad [5]$$

$$A = \frac{e\gamma_p}{Y_{v,o}} \exp(\frac{E}{RT_p}) \quad [6]$$

In this work, the estimated values for A and E are 358000 s^{-1} and 89100 kJ/kmol respectively.

3.2 Heat transfer within the solid

The 1-D heat transfer equation, which accounts for the in-depth radiation absorption with an energy source term, reads:

$$\rho c_p \frac{\partial T}{\partial t} = \frac{\partial}{\partial x}(k \frac{\partial T}{\partial x}) + \dot{q}'''_{s,c} + \dot{q}'''_{s,r} \quad [7]$$

where ρ, c_p and k are respectively the density, specific heat and conductivity of the solid. The variables $\dot{q}'''_{s,c}$ and $\dot{q}'''_{s,r}$ denote respectively a chemical and a radiative source term. Eq. [7] is solved using a uniform mesh with a cell size $\Delta x =$ 0.376 mm.

The chemical source term $\dot{q}'''_{s,c}$ is modelled using an Arrhenius expression:

$$\dot{q}'''_{s,c} = -\rho_v A Y_v \exp(-\frac{E}{RT}) H_p \quad [8]$$

where H_p is the heat of reaction in kJ/kg. A positive value of H_p means that the pyrolysis reaction is endothermic, while a negative value of H_p means that the reaction is exothermic.

The radiative absorption term $\dot{q}'''_{s,r}$ is a function of absorption coefficient (κ) and emissivity (ε).For an opaque material, the thermal radiation is absorbed within an infinitely thin layer at the solid surface, and the corresponding absorption coefficient is infinitely large. For some other materials the radiation can penetrate to some finite depth, and the absorption coefficient value is smaller than infinity.

In order to solve the radiative absorption term in the heat conduction equation, a two-flux model is employed. This model is based on the Schuster-Schwarzschild approximation [5], which assumes that the intensity is constant inside the 'forward' and 'backward' hemispheres. Accordingly, the radiative source term $\dot{q}'''_{s,r}$ is taken as the sum of the 'forward' $\dot{q}_r^+(x)$ and 'backward' $\dot{q}_r^-(x)$ flux gradients.

$$\dot{q}'''_{s,r(x)} = \frac{d\dot{q}_r^+(x)}{dx} + \frac{d\dot{q}_r^-(x)}{dx} \quad [9]$$

The forward radiative heat flux into the solid is computed as follow:

$$\frac{d\dot{q}_r^+(x)}{dx} = 2\kappa(\sigma T_{(x)}^4 - \dot{q}_r^+(x)) \quad [10]$$

A similar formula can be given for the 'backward' direction. The boundary condition for $\dot{q}_r^+(x)$ at the solid surface is given by:

$$\dot{q}_r^+(0) = \varepsilon \dot{q}''_e + (1-\varepsilon)\dot{q}_r^-(0)) \quad [11]$$

The boundary condition at the front surface of the solid reads:

$$-k \frac{\partial T}{\partial x}\bigg|_{x=0} = \varepsilon \dot{q}''_e - \dot{q}''_c - \varepsilon\sigma\left(T_s^4 - T_\infty^4\right) \quad [12]$$

On the right hand side, $\dot{q}''_e$ is the incident heat flux, $\dot{q}''_c$ is the convective heat flux. It is calculated with the following expression:

$$\dot{q}''_c = h(T_s - T_\infty) \quad [13]$$

where T_s and T_∞ are the surface temperature of the solid and the temperature of the surrounding air; h is the convective heat transfer coefficient, which is calculated based on a combination of natural and forced convection correlations.

For the back-side, a perfectly insulated condition is applied:

$$-k\left.\frac{\partial T}{\partial x}\right|_{x=h}=0 \qquad [14]$$

3.3 Thermal properties

The properties of MDF and the model parameters will be discussed in this section, including the density, thermal conductivity, specific heat, heat of pyrolysis, emissivity, and the absorption coefficient. In general, determining these parameters is challenging due to their dependency on temperature, test conditions, and uncertainties related to the measurement method.

3.3.1 Densities of virgin MDF and char

It has been reported in the literature [2, 9-11] that the density of the MDF is not uniform along the thickness of the sample, namely due to the hot-processing operation during its manufacturing. It is highest at the surface of the sample and lowest at mid-depth. The MDF density profile suggested in [2] (see parabolic profile in Fig.3) is expressed as:

$$\rho_v(x)=\frac{3\rho_{v,bulk}}{2+\xi}\left[4(1-\xi)\left(\frac{x}{h}\right)\left(1-\frac{x}{h}\right)+\xi\right] \qquad [15]$$

where the bulk density is $\rho_{v,bulk}=605$ kg/m^3 (as measured), and the ratio, ξ, of the maximum density to the minimum density in the sample panels is estimated in reference [2] to be 1.61 that also agrees with values observed in the literature, ranging between 1.50 and 1.75 [9] for different MDF panels.

Figure 3. Through-thickness density profile for both uniform density and non-uniform density cases.

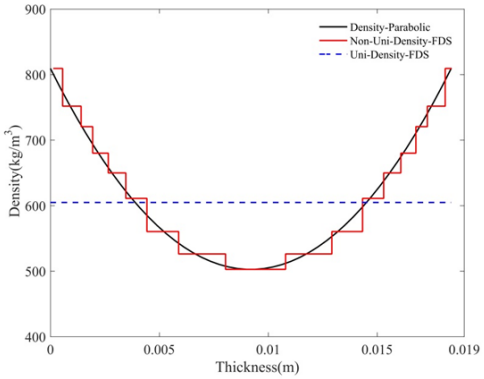

Both the uniform and non-uniform density cases have been considered in this work. In FDS, the solid can be represented with different layers, and each of the layers having its thermal properties can undergo reactions. For the non-uniform density case, 17 layers have been used to represent the sample (see Fig. 3). Each layer has a constant density. The minimum value is 502.92 kg/m^3, i.e. at the middle of the sample, while the maximum value is 809.46 kg/m^3 ,i.e. at the front and back surface.

The density of char was calculated based on the assumption that the volume of the solid sample is fixed during the burning process. Considering a value of 0.21 for the char yield [3], a char density of 127 kg/m^3 is approximated.

3.3.2 Thermal conductivity

Although the thermal conductivity depends on time-varying temperature as well as the local density and constant values are still widely used in pyrolysis models (for example [14-16]). Here, taking the range of 0.08 to 0.41 W/(m·K) for wood material as reference [13], a constant value of 0.18 W/(m·K) is considered for MDF.

The char thermal conductivity of MDF should be similar as that of softwood, since their densities are

similar. In [17, 18], the value for wood char is reported within a range of 0.05 to 0.175 W/(m·K) for temperatures between 300 K and 873 K. Since for the most time during the pyrolysis process, the sample temperatures range from 700 K to 1000 K, a constant value of 0.17 W/(m·K) is considered appropriate..

3.3.3 Specific heat capacity

The specific heat capacity of wood based materials depends on the temperature and moisture content of the material, but is independent of density and species [19]. According to a literature survey by Gronli [13], specific heat capacities used for unreacted wood material in pyrolysis models vary from 1.5 to 2.51 kJ/(kg·K), whereas Gupta et al.[18] report that values from 0.67 to 2.5 kJ/(kg·K) have been used. In this study, a constant value of 1.58 kJ/(kg·K) is considered.

The reported values in the literature for specific heat capacity of wood char range from 0.67 to 1.35 kJ/(kg·K) at room temperature [13]. If the temperature increases up to a range of 523 K – 673 K, the specific heat capacity can increase up to 1.9 kJ/(kg·K). Here, the constant value of 1.4 kJ/(kg·K) is used.

3.4 Heat of pyrolysis

The heat of wood pyrolysis reported in the literature [21] ranges from endothermic (370 kJ/kg) to large exothermic values (-1700 kJ/kg), depending on the experimental conditions. The heat of pyrolysis is not available for MDF used in this study. Here a value of 0 kJ/kg is first considered and other possible values will be discussed in the sensitivity study.

3.5 In-depth radiation parameters

The values for the emissivity and absorptivity are assumed to be the same in FDS by default. It has been reported in [1] that the effective emissivity of virgin material is a function of temperature. For a temperature range up to 1500 K, the corresponding emissivity ranges from 0.6 to 0.9. The effective emissivity of char, as reported in [1], is approximately0.86 and relatively independent of temperature over a wide temperature range (300-3000K). In the base case, values of 0.86 for both the virgin and char emissivity have been used.

The absorption coefficient of MDF, κ , has been hardly mentioned or discussed in the literature. However, for polymeric materials such as PMMA, it has been investigated in the literature. In [5] a wide range of possible values for κ (from 333 m^{-1} to 2000 m^{-1}), is examined for black PMMA. In our study, first the default FDS value of 50000 m^{-1} is considered for both the virgin material and char, which is deemed suitable for opaque materials. As a consequence, the in-depth radiation is effectively not considered in the equations. Table 1 shows the summary of input parameters used in the base case.

Table 1 summary of input parameters for base case as well as the optimized case.

Parameter	Unit	Base case	Optimized case	Range
Density of virgin MDF	[$kg.m^{-3}$]	605	non-uniform	-
Density of char	[$kg.m^{-3}$]	127	127	-
Residual fraction	-	0.21	0.21	-
Moisture content	[%]	0	6	-
Heat capacity of virgin MDF	[$kJ.kg^{-1}.K^{-1}$]	1.58	1.58	[0.67, 2.5]
Heat capacity of char	[$kJ.kg^{-1}.K^{-1}$]	1.4	1.4	[0.67, 1.9]
Thermal conductivity of virgin MDF	[$W.m^{-1}.K^{-1}$]	0.18	0.18	[0.08, 0.41]
Thermal conductivity of char	[$W.m^{-1}.K^{-1}$]	0.17	0.17	[0.05, 0.18]
Emissivity of virgin MDF	[-]	0.86	0.6	[0.6, 0.9]
Emissivity of char	[-]	0.86	0.86	-
Heat of pyrolysis	[$kJ.kg^{-1}$]	0	0	[-1700, 370]
Reaction order	[-]	1	1	-

Pre-exponential factor	[s^{-1}]	3.58×10^{5}	3.58×10^{5}	-
Activation Energy	[$J.mol^{-1}$]	8.91×10^{4}	8.91×10^{4}	-
Absorption coefficient for virgin	[m^{-1}]	50000	50000	-
Absorption coefficient for char	[m^{-1}]	50000	2000	-

4. SMALL-SCALE SIMULATION RESULTS

First, the values for input parameters in Table 1 are applied in the simulations, which is the base case simulation. These results of this simulation case, including mass loss rate and front surface temperature, are presented in the following section.

Moreover, a sensitivity study has been conducted for the different model parameters, namely, for the thermal conductivity, specific heat capacity, heat of pyrolysis, emissivity, through-thickness density profile, and absorption coefficient. Consequently, a set of 'optimized' parameters have been determined through a simple trial and error procedure, shown in Table 1 as the optimized parameters.

4.1. Base case simulation results

4.1.1. Mass loss rate

The mass loss rate results are presented in Fig.4 (a-c). Three external heat flux values have been considered, namely 100, 50, and 25 kW/m^2.

There are two peaks in the mass loss rate curves for different external heat flux values. The first peak arises due to a high temperature reached at the surface. After the pyrolysis process, a char layer is formed at the surface of the sample. This insulating char layer decreases the gasification rate. As a result, the mass loss rate drops to a lower level. The second peak is mainly due to the heat accumulation at the back side.

The simulated values for the first peak are significantly lower than the measured values with relative deviations of about 21%, 50% and 63 % for respective heat flux exposures of 25, 50, and 100 kW/m^2. Furthermore, the time to reach the first peak is shorter in the predicted profiles by about 34 s, 107 s and 381 s for respective heat flux exposures of 25, 50, and 100 kW/m^2. Deviations are particularly pronounced for the lower external heat flux value (25 kW/m^2). One possible reason could be that the one-step reaction is too strong a simplification for the complex phenomena taking place during the pyrolysis process. The consequence of possible shortcomings in the chemistry is expected to be more pronounced as the pyrolysing zone occupies a larger volume in the material, which is the case for lower heat fluxes. Fig. 3(d) illustrates this, showing the through-thickness temperature evolution for heat flux values of 100 and 25 kW/m^2. The thickness in the solid occupied by temperature range [200°C - 400°C], corresponding to the pyrolysing zone (Fig. 2), is indeed much wider for 25 kW/m^2 than for 100 kW/m^2 (0.0081m and 0.0022 m respectively).

Figure 4. Comparisons between experimental data and predicted results for (a) MLR at 100kW/ m^2, (b) MLR at 50kW/ m^2 (c) MLR at 25kW/ m^2 and (d) through-thickness temperature at exposures of 100 and 25 kW/ m^2.

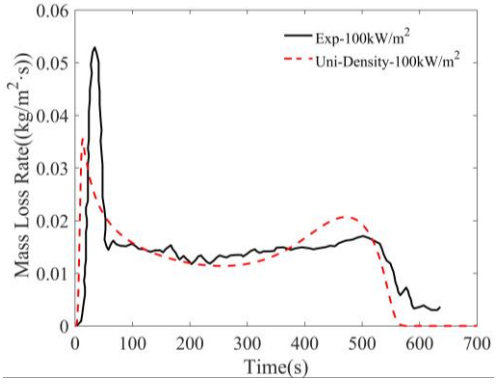

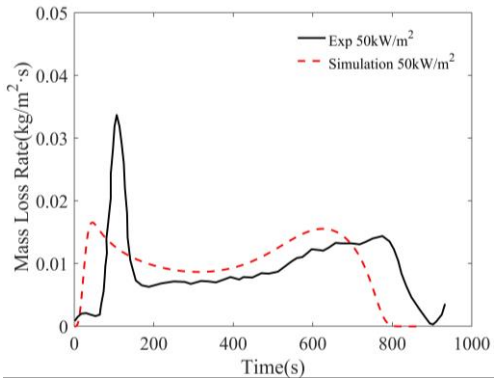

(a) (b)

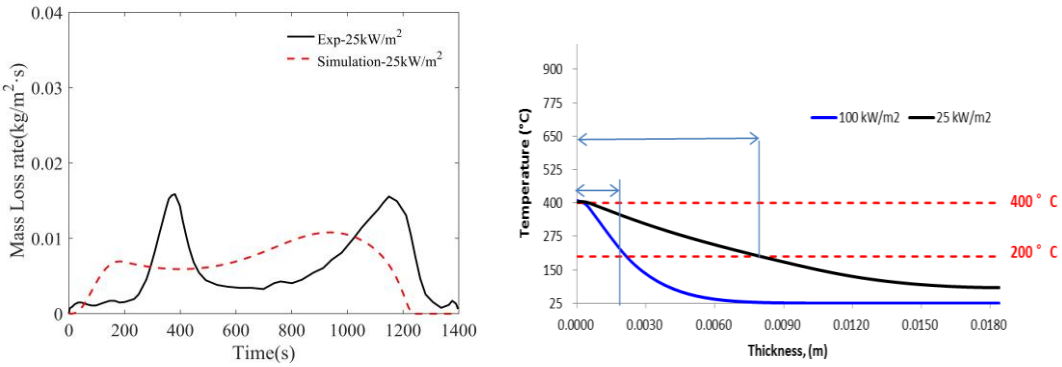

(c) (d)

In order to quantitatively indicate the difference between the experimental data and the predicted results, the time, t_p, to reach the peak, as well as the value of the peak, $\dot{m}''_p$, are listed in Table 2. For the time to reach the peak MLR, the predicted values are much smaller than the experimental results, namely by about 50 to 65%). For the value of the peak, larger deviations are observable for lower heat flux exposures.

Table 2 Characteristic values of t_p and $\dot{m}''_p$ from the experiments and the predictions with FDS.

Cases	t_p-exp(s)	t_p-sim (s)	ε_{tp}	$\dot{m}''_p$-exp(kg/(sm^2))	$\dot{m}''_p$-sim(kg/(s/m^2))	ε_{mp}
100 kW/m^2	34.3	12.0	-65.0%	0.052	0.041	-21.1%
50 kW/m^2	106.8	40.8	-61.8%	0.034	0.017	-50.0%
25 kW/m^2	380.8	186.0	-51.1%	0.016	0.006	-62.5%

4.1.2. Front temperature

The experimental and simulated results for the surface temperature are shown in Fig.5. The temperatures are overpredicted during the initial heating-up period, roughly in the first 70s, 130s, and 400s at heat flux rxposures at 100, 50, and 25 kW/ m^2. This is in accordance with the MLR results displayed in Fig.4. After the initial heating-up period, the temperature results for the heat flux exposures at 100 and 50 kW/m^2 cases are well predicted. However, the temperature at the end of the 25 kW/m^2 case is slightly underpredicted.

Figure 5. Surface temperature comparison between the experiment and simulation for three heat flux exposures.

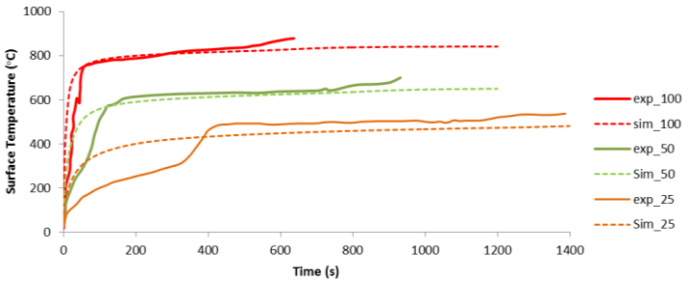

4.2. Influence of input parameters

A sensitivity analysis has been conducted to check the influence of the input parameters on the burning behavior. These parameters include the thermal properties of MDF, namely the conductivity, the specific heat capacity, the heat of reaction, moisture content, emissivity, and the absorption coefficient. The range of these parameters has been determined based on the values reported in the literature, while the applied external heat flux is 50 kW/m^2.

4.2.1. Influence of specific heat capacity

A sensitivity analysis has been conducted for evaluating the influence of the specific heat capacity. Three values have been investigated, namely 1, 1.5, and 2 kJ/(kg·K). The results are illustrated in Fig. 6. With a higher specific heat capacity, more time is required to reach the first peak (e.g., 14 % difference between 1.5 and 2 kJ/(kg.K). Furthermore, the peak value is significantly lower (e.g., 28 % difference between 1.5 and 2 kJ/(kg.K). Moreover, the front surface temperature for the higher specific heat capacity case is lower than that of the case with lower heat capacity value.

Figure 6. Influence of specific heat on the (a) mass loss rate and (b) surface temperature.

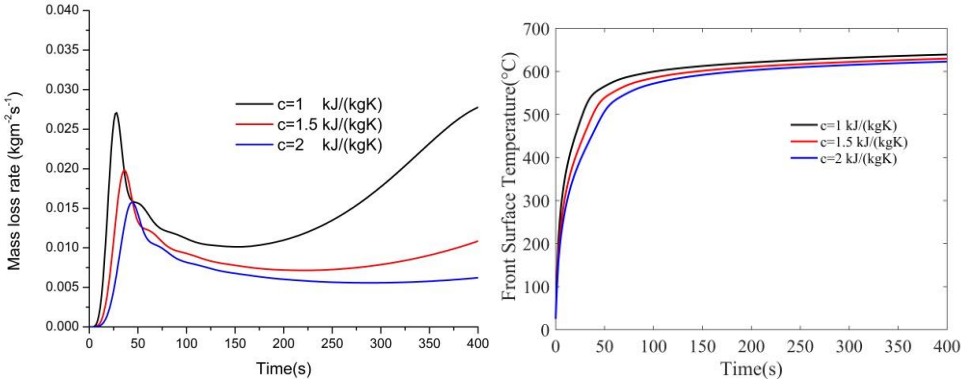

(a) (b)

4.2.2. Influence of thermal conductivity

A separate sensitivity analysis has been conducted for the thermal conductivity. Three values have been investigated, namely 0.3, 0.2, and 0.1 W/(m·K). The results are demonstrated in Fig.7. When increasing the thermal conductivity, the thermal diffusivity ($k / \rho c$) increases. Thus, heat can penetrate deeper into the material in the same time period, thus the pyrolysis process at the surface is slow down during the initial heating-up period.

Figure 7. Influence of thermal conductivity on the (a) mass loss rate and (b) surface temperature.

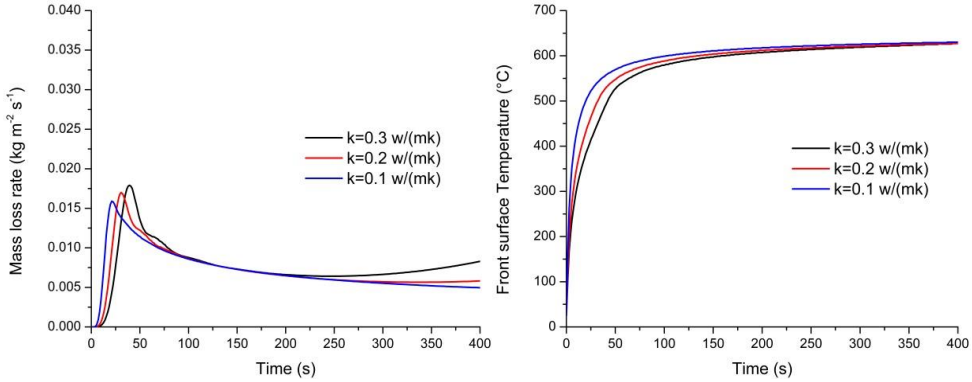

(a) (b)

When increasing the thermal conductivity of the virgin material from 0.1 W/(m·K) to 0.3 W/(m·K), the time to reach the peak increases by 31.8% and the value of the peak increases by 6.4%. Moreover, the surface temperatures take more time to reach the experimental values when the conductivity is higher, as heat is conducted into the material more easily.

4.2.3. Influence of the heat of pyrolysis

The heat of pyrolysis does not have a significant influence on the pyrolysis process. Increasing H_p from 0 to 100 kJ/kg results in differences less than 5% in the mass loss rates and the front surface temperatures.

4.2.4. Influence of the moisture content

Moisture content (MC) is a measure of the amount of water within a material. MC is expressed as the percentage of the mass of the material that contributes water content. In this study, the original MC of the sample was approximately 6%.

In order to check the influence of the MC, a second Arrhenius equation for the water evaporation was added. Again Eqs. 2, 3, and 4 were employed to estimate the kinetic parameters *A* and *E*. The peak reaction rate $\gamma_p = 0.0016\,\mathrm{s}^{-1}$ occurs at a temperature $T_p = 100\,°\mathrm{C}$. A value of 5 K/s is used for the heating rate. Three MC values have been considered, namely 0, 5, and 10%. The comparison of simulation results is displayed in Fig. 8.

Figure 8. Influence of MC on the simulated (a) mass loss rate and (b) surface temperature.

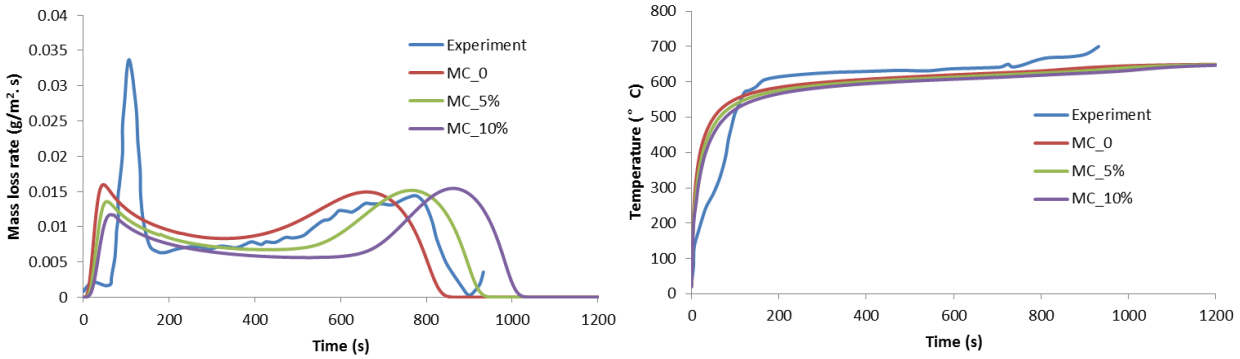

(a) (b)

Increasing the MC from 0 to 5%, the peak value $\dot{m}''_p$ decreases by 16.73%, while the time to reach the first peak t_p increases by 17.53%. Moreover, the overall reaction time increases by 20%. This influence can be explained in terms of the amount of energy required for the evaporation process, i.e. more water or moisture content means that the sample needs more energy for water evaporation. Obviously, the MC has a significant influence on the burning behaviour. The optimized value of 6% MC will be used hereafter.

Up to this point, the results of the aforementioned sensitivity analysis show that the most significant influence on the peak value for the mass loss rate is caused by the specific heat capacity. Nevertheless, none of these results showed satisfactory results for the time to reach the peak value of the burning rate when compared to experimental data, namely, the predicted time to peak is significantly lower than the measured value.

4.2.4. Influence of the emissivity

In light of the above, another sensitivity analysis has been conducted for the effective emissivity of virgin. The considered range of the emissivity rangs from 0.5 to 0.8. The comparisons are shown in Fig. 9. For the boundary condition, we are assuming the absorptivity is equal to the emissivity. When decreasing the emissivity (thus also absorptivity), less energy is received at the sample surface. Therefore, more time is required to reach the first peak in MLR and thus the maximum front surface temperature.

Figure 9. Influence of emissivity on the (a) mass loss rate and (b) surface temperature.

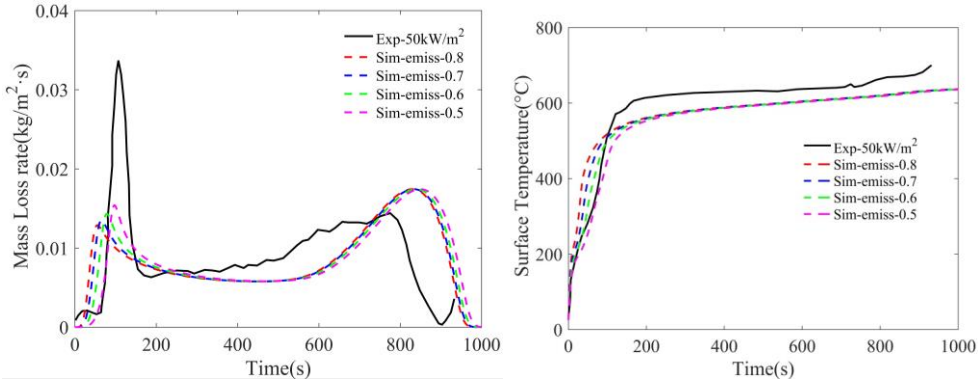

(a) (b)

When decreasing the emissivity of virgin from 0.86 to 0.6, the time to reach the first peak increases by 116%, and the peak value increases by 11.24%. Based on these results, a value of 0.6 for the emissivity of the virgin material is suggested. Consequently, emissivity can be identified as the first parameter that plays a role in the timing of the peak mass loss rate.

4.2.5. Influence of the absorption coefficient

Figures 10 and 11 display the results for the influence of the absorption coefficient on the mass loss rate (a) and front surface temperature (b), fixing the emissivity of the virgin material at 0.6, and the emissivity of char at 0.86. In general, both the absorption coefficient of virgin and char have significant influence on the mass loss rate curve. In Fig. 10, when decreasing the values of the absorption coefficient of virgin from 50,000 m^{-1} to 30 m^{-1} leads to a significant increase in the peak MLR and a delay in the time to reach the peak. Specifically, the values of the absorption coefficient of virgin between 30 m^{-1} and 700 m^{-1} show the most significant influence. The peak value is improved by 48.25%, and the time to reach the first peak is improved by 18.42%.

Figure 10. Influence of absorption coefficient of virgin on the (a) mass loss rate and (b) surface temperature.

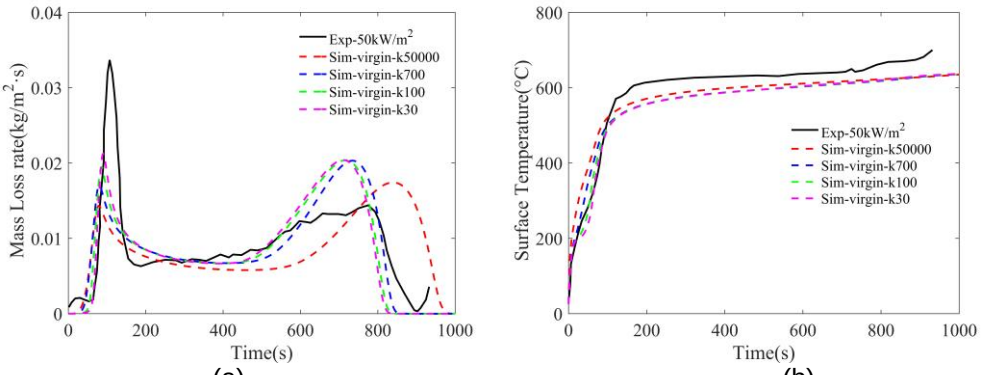

(a) (b)

Figure 11. Influence of absorption coefficient of char on the (a) mass loss rate and (b) surface temperature.

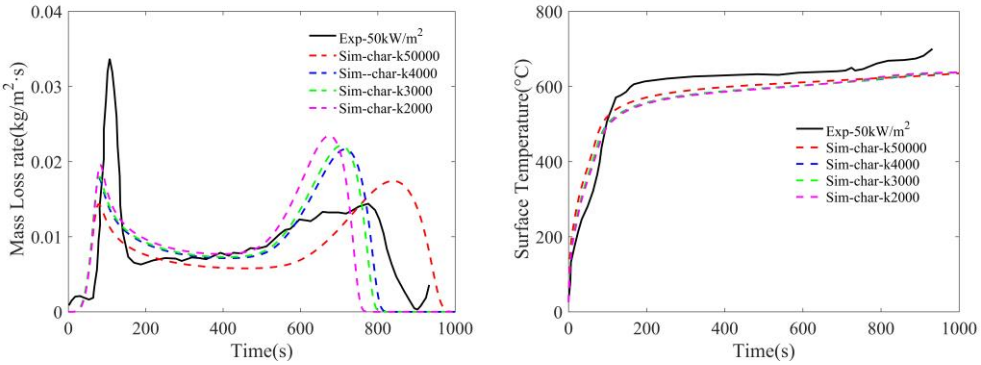

(a) (b)

As indicated in Fig. 11 (a), the considered range of the absorption coefficient of virgin between 2000 m^{-1} and 4000 m^{-1} shows significant influence. The peak value is increased by 39%, while the time to reach the first peak is not improved very noticeably. Furthermore, the absorption coefficient of char has significant influence on the second peak. This could be explained by fact that the top layers of the sample are covered with char. And with the increase of the absorption coefficient of char, the radiation can penetrate deeper into the sample, which accelerates the reaction. Thus the overall reaction time decreases. However, this does not significantly influence the surface temperature, as shown in Fig 11 (b).

As mentioned in the introduction, the in-depth-like radiation absorption may occur in case of cracks or delamination. Hence, it is reasonable to assume that the material is opaque until it starts charring. Based on this consideration, values of 50000 m^{-1} and 2000 m^{-1} are suggested for the absorption coefficient of virgin and char, respectively.

This finding should be taken into account with caution and must be further investigated. It highlights, nevertheless, the possible importance of in-depth radiation in the pyrolysis modelling of MDF and more generally wood-based materials.

4.2.6. Non-uniform through-thickness density profile

As mentioned in the previous section, the density is not uniform through the sample thickness. In fact a high density value is observed on the surface. With a higher density, a higher peak value is expected. The non-uniform through-thickness density profile used here is the one mentioned in section 3.3.1. The results are shown in Fig. 12. Two heat flux values have been considered here.

Figure 12. Influence of the through -thickness density profile on the mass loss rate for heat flux exposures of (a) 50 kW/m^2, (b) 25kW/m^2.

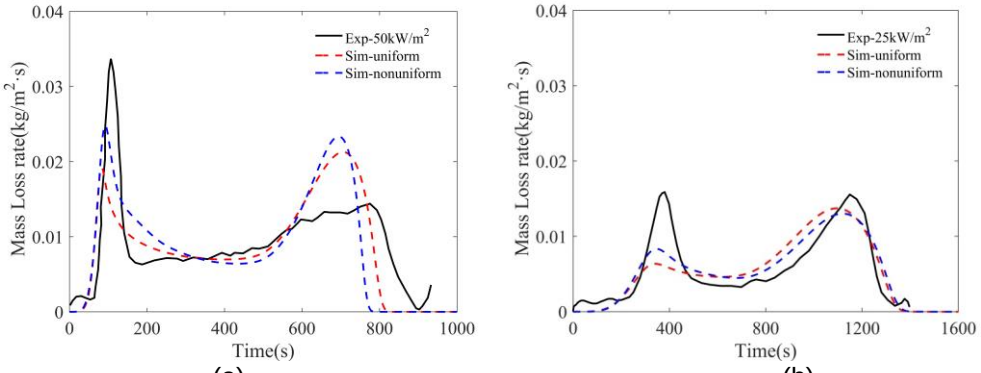

(a) (b)

It is notable that, the first peak is significantly improved by 29.84% for 50 kW/m^2 and by 31.74% for 25 kW/m^2 when a non-uniform density profile is applied. Therefore, a non-uniform density profile is

suggested for the optimized case.

The impact of parameter variations on t_P (time to peak mass loss rate) and $\dot{m}_p''$ (peak mass loss rate) is quantitatively shown in Table 3 for cases with 50 kW/m^2 heat flux exposure. For the considered range of the parameters, the most significant influence on the time to the first peak comes from the emissivity, followed by the thermal conductivity, specific heat, and moisture content. For the peak mass loss rate, the most significant influence comes from the absorption coefficient, followed by the through-thickness density, the moisture content, and finally the specific heat capacity.

Table 3 The impact of parameter variations on t_P and $\dot{m}_p''$

Parameter	Original Value	Changed value	dt_p(%)	$d\dot{m}_p''$ (%)
Specific Heat capacity of virgin	1.5	2	27.62	-14.47
Thermal conductivity of virgin	0.2	0.1	31.80	6.40
Absorption coefficient of char	50000	2000	8.00	39.00
Heat of pyrolysis	100	50	0	-4.91
Emissivity	0.86	0.6	116.00	11.24
Moisture content	0%	5%	17.53	16.73
Density	uniform	Non-uniform	0	29.84

4.3. Optimized values for parameters and corresponding results

In order to achieve a better estimation of the burning behavior for MDF material, a simple trial and error optimization procedure has been followed to predict the MLR from the experiment. Consequently, a set of parameters has been obtained (see Table 1), and these simulation results are demonstrated in this section as well.

Figures13 shows the simulation results using these optimized values of parameters. These results include the mass loss rate and the front surface temperature for three different external heat flux exposures. In general, as expected a better agreement is achieved when using optimized values of model parameters. For the predictions of the mass loss rate, the onset of the pyrolysis was well captured, and significant improvements were also achieved in terms of the value of the first peak in the mass loss rate curve. For the front surface temperature, the predictions of the initial heating-up period (roughly in the first 70s, 130s, and 400s at the heat flux exposures of 100, 50, and 25 kW/m^2 respectively) were notably improved and fit the experimental data better than those in the preliminary simulations.

Figure 13. Comparisons between experiment and simulation using optimized parameter values (a) mass loss rate, (b) surface temperature.

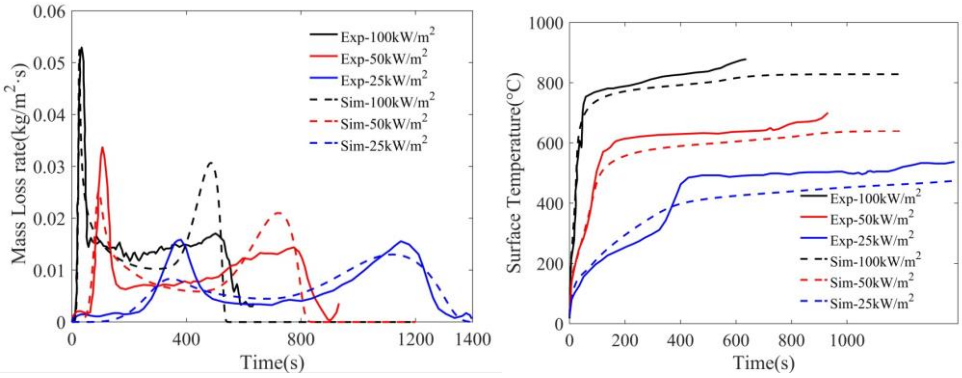

(a) (b)

CONCLUSIONS

In this work, pyrolysis behaviour of the MDF material has been studied numerically using a one-dimensional heat transfer solver, and a one-step Arrhenius type pyrolysis model. The numerical simulation tool used in this study is the Fire Dynamics Simulator (FDS 6.2.0). Within this model, the in-depth radiation has been taken into consideration. The values of the kinetic parameters and char yield are estimated from TGA test results reported in [3]. The thermal properties of virgin MDF and char are taken from the literature for the base case. It is assumed that no shrinkage and swelling occur during the whole process.

The base case does not show satisfactory results for the time to reach the first peak and the value of that peak in the mass loss rate curve when compared to experimental data. The predicted time to peak and the value of that peak are significantly lower than the measured value, namely by about 50 to 62%). The influence of the material properties and model parameters on the pyrolysis behaviour of MDF has been investigated in detail through a sensitivity analysis. The parameters include thermal conductivity, specific heat, heat of reaction, the emissivity, absorption coefficient, moisture content, and through-thickness density profile.

Based on the results of the sensitivity analysis study, it can be concluded that the main parameters influencing the t_p are the emissivity, thermal conductivity, specific heat, and moisture content. For the peak mass loss rate, the absorption coefficient of char, through-thickness density, moisture content, specific heat of virgin, and emissivity are the parameters showing most significant influence. Hence, only when proper values of the parameters were employed in the simulation, the onset of the pyrolysis process can be reasonably predicted.

Through a simple trial and error procedure, a set of ‘optimized’ parameter values has been obtained (see Table 1). During this optimization procedure, the parameters showing significant influence have been considered, including the in-depth radiation, which shows better agreement with experimental data.

ACKNOWLEDGEMENT

The authors would like to thank the China Scholar-ship Council (CSC) and BOF co-funding from Ghent University for their financial support to the first author, Grant NO.201306420001. Dr. Tarek Beji is a Postdoctoral Fellow of the Fund for Scientific Research-Flanders (Belgium).

REFERENCES

1. Marcos Chaos. Spectral aspects of bench-scale flammability testing: application to hardwood pyrolysis. pp. 165-178. Fire safety science proceedings of the Eleventh International Symposium, 2014.

2. Agarwal, G., Chaos, M, Wang, Y. Zeinali, D., and Merci, B., Pyrolysis Model Properties of Engineered Wood Products and Validation Using Transient Heating Scenarios, Interflam 2016, 14th International Conference and Exhibition on Fire Science and Engineering, Royal Holloway College, UK, 2016.

3. Kai-Yuan Li, Xinyan Huang, etc. Pyrolysis of Medium-Density Fiberboard: Optimized Search for Kinetics Scheme and Parameters via a Genetic Algorithm Driven by Kissinger’s Method. Energy & Fuels. Combustion 2014, 28 6130-6139.

4. Florian Kemple, B. Schartel, G.T. Linteris, A. Hofmann-Böllinghaus. Prediction of the mass loss rate of polymer materials: Impact of residue formation. Combustion and Flame 159(9):2974-2984.September 2012.

5. Nicolas Bala, Guillermo Rein. On the effect of inverse modelling and compresation effects in computational pyrolysis for fire scenarios. Fire safety journal Volume 72, February 2015, Pages 68–76.

6. Fenghui Jiang, J.L. de Ris, M.M. Khan b. Absorption of thermal energy in PMMA by in-depth

radiation. Fire Safety Journal 44 (2009) 106– 112.

7. Gregory Linteris, etc. Absorption and reflection of infrared radiation by polymers in fire-like environments. Fire and Materials, 2012.

8. McGrattan, K., Randall McDermott, etc. Fire dynamics simulator user's guide, National Institute of Standards and Technology Report NIST special publication 1019. (2016).

9. Wang, X., Mohammad, M., Hu, L.J., Salenikovich, A., Evaluation of density distribution in wood-based panels using X-ray scanning, *Proceedings of the 14th International Symposium on Nondestructive Testing of Wood*, University of Applied Sciences Eberswalde, Germany, 2005.

10. MDF material manufacturer : http://www.spanolux.com/en.

11. Kaiyuan.Li etc. Determining thermal physical properties of pyrolyzing new Zealand medium density fibreboard. Chemical engineering science 95 (2013) 211-220.

12. Cai, Z., Muehl, H.J., Winandy, J.E., Effects of pressing schedule on formation of vertical density profile for MDF panels, 40th International Wood Composites Symposium, Seattle, Washington, 2006.

13. Gronli, M.G. Theoretical and experimental study of the thermal degradation of biomass. Doctoral dissertation. Trondheim. Norwegian University on Science and Technology, Faculty of Mechanical Engineering, Dept. of Thermal Energy and Hydropower. Norway.p339.

14. Wang,X., Kersten, S.R.A., Prins, W.P.m. Biomass pyrolysis in a fluidized bed reactor. Part 2: Experimental validation of model results. Industrial &Engineering Chemistry Research. 2005. Vol.44 pp. 8786-8795.

15. Younsi, R., Kocaefe, D., Poncsak, S. and Kocaefe, Y. Thermal modelling of the high temperature treatment of wood based on Luikov's approach. International Journal of Energy Research. 2006. Vol.30, pp.699-711.Franks, C., Fire and Materials 2017, Interscience Communications Ltd, London, UK, p1- p2.

16. Saastamoinen, J., Simplified model for calculation of devolatilization in fluidized beds. 2006. Fuel. Vol. 85, pp. 2388-2395.

17. Brown, L. E.. An experimental and analytical study of wood pyrolysis. Doctoral dissertation. The University of Oklahoma.1972.

18. Gupta, M., Yang, J., Roy. C. Specific heat and thermal conductivity of softwood bark and softwood char particles. Fuel. Vol. 82, pp. 919-927.2003.

19. Simpon, W. and TenWolde, A. Physical properties and moisture relations of wood. In Forest products laboratory. 1999. Wood handbook.-Wood as an engineering material.

20. Siau, J.F. Transport process in wood. Springer-verlag, Berlin. 1984.

21. A.F. Roberts. The heat of reaction during the pyrolysis of wood. Combustion and Flame. Vol 17 pp. 79-86. 1071.

22. D. Zeinali, etc. Computational analysis of pyrolysis and flame spread for MDF panels placed in a corner configuration. 8th ISFEH Proceedings, (2016).